

1N-24-TM
134077

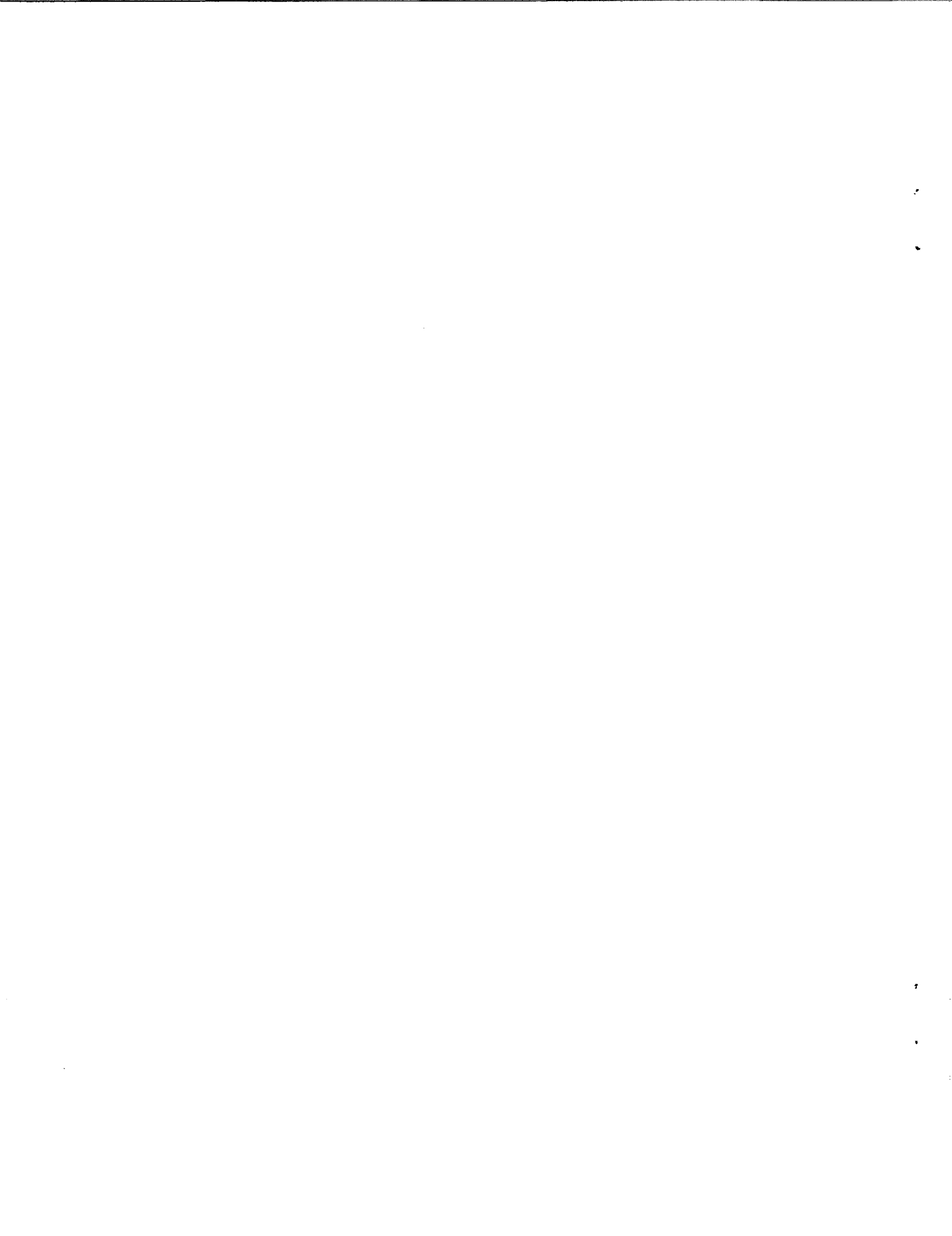
EFFECT OF CURVATURE ON THE IMPACT DAMAGE CHARACTERISTICS AND
RESIDUAL STRENGTH OF COMPOSITE PLATES

Damodar R. Ambur and James H. Starnes, Jr.
NASA Langley Research Center
Hampton, VA

Presented at the 39th AIAA/ASME/ASCE/AHS/ASC Structures,
Structural Dynamics, and Materials Conference

AIAA Paper No. 98-1881

Long Beach, California
April 20-23, 1998



EFFECT OF CURVATURE ON THE IMPACT DAMAGE CHARACTERISTICS AND RESIDUAL STRENGTH OF COMPOSITE PLATES

Damodar R. Ambur* and James H. Starnes, Jr.[†]
 NASA Langley Research Center
 Hampton, VA

Abstract

The results of a study of the response and failure characteristics of thin, cylindrically curved, composite plates subjected to low-speed impact damage are presented. The results indicate that the plate radius and the plate thickness are important structural parameters that influence the nonlinear response of a plate for a given amount of impact energy. Analytical and experimental contact-force results are compared for several plates and the results correlate well. The impact-energy levels required to cause damage initiation and barely visible impact damage are a function of the plate radius for a given plate thickness. The impact-energy levels required to initiate impact damage for plates with a certain range of radii are greater than plates with other radii. The contact-force results corresponding to these impact-energy levels follow a similar trend. Residual strength results for plates with barely visible impact damage suggest that the compression-after-impact residual strength is also a function of plate radius. The residual strength of impact-damaged flat plates appears to be lower than the residual strength of the corresponding cylindrically curved plates.

Introduction

The effect of low-speed impact damage on the compression strength of laminated composite structures has been studied extensively by many researchers over the past several years. Test data show that the compression strength of composite structures can be

significantly reduced by low-speed impact damage, even if the damage is not detectable by visual inspection. Most of the studies of the effects of low-speed impact damage reported in the literature have focused on thicker flat plates that are typical of those used for wing structures. There is very limited information in the literature that addresses the low-speed impact response of thinner curved composite plates that are typical of fuselage skins. Composite fuselage structures usually have skins that are 16-ply thick or less. It has been shown that these thinner composite skins will experience large deformations when subjected to the transient normal force associated with a low-speed impact event, even for low impact-energy levels.¹⁻⁴ It has also been shown that structures with curvature and certain combinations of plate dimensions exhibit a nonlinear softening response when impacted with dropped-weight impactors.⁵⁻⁷ A geometrically nonlinear analysis method based on Lagrangian equations of motion and the Rayleigh-Ritz method with assumed mode shapes was developed to predict the nonlinear response of cylindrically curved composite plates, and the results from this analysis have been correlated with experimental results.⁸ These results indicate that the stiffness of curved composite plates decreases as the dropped-weight impact event progresses. This stiffness reduction suggests that the impact-damage characteristics of curved composite plates can be significantly different from the response of flat composite plates. Since the response of flat composite plates subjected to a low-speed impact event from an airgun-propelled impactor is different from the response of a flat plate subjected to a dropped weight, it is important to identify the differences in the response of a curved composite plate subjected to a low-speed impact event from both an airgun-propelled impactor and from a dropped weight. The effect of any resulting impact damage on the residual strength of a composite plate is usually determined from the results of compression-after-impact tests. Understanding the nature of the

* Assistant Head, Structural Mechanics Branch, Associate Fellow, AIAA.

[†] Head, Structural Mechanics Branch, Fellow, AIAA.

Copyright © 1998 by the American Institute of Aeronautics and Astronautics, Inc. No copyright is asserted in the United States under Title 17, U.S. Code. The U.S. Government has a royalty-free license to exercise all rights under the copyright claimed herein for government purposes. All other rights are reserved by the copyright owner.

structural responses, damage characteristics, and residual strength of curved composite plates as a function of impactor and structural parameters is essential for designing safe, weight-efficient, and cost-effective curved composite structures.

The present paper presents the results of a study of the effect of low-speed impact events on the response and residual strength of thin, cylindrically curved, quasi-isotropic graphite-epoxy plates with different radii and thicknesses. The influence of curvature on the impact response of the plates and the impact-energy levels necessary to cause damage initiation and barely visible damage are discussed. A barely visible impact damage criterion is identified, and residual-strength results based on this criterion are presented and discussed for 8- and 16-ply-thick, cylindrically curved, quasi-isotropic composite plates.

Test Specimens and Test Procedure

The test specimens studied in this investigation were fabricated from Hercules, Inc. AS4 graphite fibers preimpregnated with Hercules, Inc. 3502 epoxy resin. The specimens were cured using the resin manufacturer's recommended curing procedure. Typical mechanical properties for the AS4-3502 graphite-epoxy material are presented in Table 1. The nominal ply thickness of the material is 0.005 in. Specimens were fabricated to form 8- and 16-ply-thick flat and curved plates with $[45/0/-45/90]_n$ laminates, where n is equal to 1 or 2, respectively. The curved specimens have 15-, 30-, and 60-in. radii. Both the flat and curved specimens are 5-in. wide and 9-in. long.

The specimens were supported with clamped boundary conditions using a test fixture described in Ref. 8, and subjected to a normal impact force by an airgun-propelled impactor or a dropped weight. An instrumented 2.5-lb steel weight with a 0.5-in.-diameter hemispherical tip was used for the dropped-weight impactor. A 0.5-in.-diameter aluminum sphere was used for the airgun-propelled impactor. The dropped-weight impactor was dropped from a prescribed height, and the airgun-propelled impactor was propelled by compressed air with a prescribed speed to impact the specimens with a prescribed impact-energy level.

The impact-energy levels were increased from a low level to determine the impact energy necessary to initiate damage in the specimens, and to cause barely visible damage on the surface of the specimens. The compression-after-impact residual strength of the impact-damaged specimens was determined by testing the specimens in a 120-kip hydraulic test machine. For these tests, the longitudinal, unloaded edges of the

specimens were simply supported using knife edge supports, and the loaded edges were clamped. Electrical resistance strain gages and displacement transducers were used to measure specimen response as the load was applied. A shadow moiré interferometry technique was used to monitor the out-of-plane displacements of the specimens during the tests.

Results and Discussion

Contact force test results are presented in this section for flat and cylindrically curved composite plates that were impacted by dropped weights with impact-energy levels that do not initiate damage in the plates. These results are compared with analytical results for curved plates impacted with dropped weights and airgun-propelled impactors with the same impact-energy levels to identify the differences in the response of the plates for airgun-propelled and dropped-weight impactors. Impact-damage initiation and barely visible impact-damage threshold-energy results are also presented, and the effects of varying plate radius and thickness on these results is discussed. Compression-after-impact residual-strength results are presented for plates with barely visible impact damage, and a criterion based on these results is also presented. The effects of varying plate radius and thickness on these results are discussed.

Contact Forces

The maximum values of the contact forces measured by the instrumented dropped-weight test apparatus are shown in Fig. 1 for 16-ply-thick plates with different radii and impacted with 1.5 ft-lb of impact energy. The experimental results are shown in the figure by the open circles and the corresponding analysis results from the analysis of reference 8 are shown by the open squares. The flat plate results are presented in this figure against a plate radius of 200 inches. These results indicate that the value of the contact force decreases significantly for radii between 15 and 60 inches, and then increases to a value that closely corresponds to the flat-plate contact-force result for radii greater than 60 inches. These results suggest that the curved plates have a nonlinear response for radii less than 60 inches. These experimental and analytical contact-force results for dropped weights compare well. Analytical results from the analysis of reference 8 are shown in the figure by the open triangles for the airgun-propelled impactors with 1.5 ft-lb of impact energy level. The magnitudes of these contact forces are significantly greater than the contact forces for the dropped weights, and the radius of the plate has an

insignificant influence on the value of the contact forces. Apparently, the high-speed transient nature of the airgun impact event results in a very local response of the plate which does not affect the value of the contact forces for the plates considered in this study.

Impact-Damage-Initiation and Barely Visible Impact-Damage Energies

The differences in the contact-force magnitudes described in the previous section influence the damage characteristics of the plates. The damage-initiation impact-energy levels for curved plates were determined by impacting a given specimen with impact-energy levels that were increased in increments of 0.25 ft-lb until damage initiation occurred. Damage initiation was determined nondestructively using the volumetric scanning approach outlined in Ref. 6. The damage-initiation results for the 16-ply-thick $[45/0/-45/90]_2s$ quasi-isotropic plates impacted with dropped weights and airgun-propelled impactors are presented in Fig. 2 for different radii by the open circles and open squares, respectively. The impact energy required to initiate damage is significantly greater for the dropped weights than that of the airgun-propelled impactors. As the plate radius increases to a value of approximately 30 inches, the impact energy required to initiate damage increases, and then decreases for larger radii for both the airgun-propelled and dropped-weight impactors. The dropped-weight impact-energy results are consistent with the trend of the maximum contact-force results presented in Fig. 1, which suggests that a greater impact-energy level is needed for the 30-in.-radius plates to generate the impact force required to initiate damage than for other plates considered in this study. The trend for airgun contact-force results presented in Fig. 1 is not consistent with the nonlinear damage-initiation impact-energy results trend as the plate radius increases. The damage-initiation results presented in Fig. 2 suggest that the damage-initiation mode associated with the much larger contact forces for the airgun-propelled impactors could be different from those of the dropped weights for plates with different radii, and might be responsible for the observed nonlinear trend in the damage-initiation results.

The impact-energy levels required to cause barely visible impact damage on the impacted and opposite or back surfaces of 16-ply-thick plates were determined by increasing the airgun and dropped-weight impact-energy levels until damage was visible on one or both plate surfaces. Typical damage modes for the impacted and back surfaces of 16-ply-thick flat and 15-in.-radius curved plates impacted with dropped weights are shown

in Figs. 3 and 4. The impact event causes a dent to form on the impacted surface of the plate at the impact site, and causes the surface ply on the back surface of the plate opposite to the impact location to crack and separate from the plate as shown in the figures. These observations indicate that barely visible impact damage can be detected when the measured dent depth on the impacted surface is approximately 0.05 in. for the 16-ply-thick specimens for both the airgun-propelled and dropped-weight impactors. The dropped-weight impact-energy results presented in Fig. 5 suggest that greater impact-energy levels are needed to develop visible damage in both the 8- and 16-ply-thick curved plates with radii between 15 and 60 in. The measured contact-force results that correspond to these impact-energy levels are shown in Fig. 6. The trends for these contact-force results are similar to those for the impact-energy results. The airgun impact-energy level needed to develop barely visible impact damage is a constant of approximately 9.0 ft-lbs over the range of plate radii considered as indicated in Fig. 5. For the 8-ply-thick plate (0.044-in. thick) the 0.05 in. dent depth does not result in a through penetration. The damage modes for the 16-ply-thick, 15-in.-radius curved plates that were impacted with airgun-propelled and dropped-weight impactors with 8.5 ft-lbs of impact energy are shown in Fig. 7. The damage due to the airgun-propelled impactor is more severe at the impact site than that of the dropped-weight impactor. The airgun-propelled impactor causes all of the plies to fail through the plate thickness, but the dropped-weight impactor only causes extensive delaminations in the plate. The results presented in Fig. 5 suggest that radius is an important structural parameter that must be considered when assessing the damage tolerance of thin, cylindrically curved plates.

Compression-After-Impact Residual Strength

To determine the residual strength of impact-damaged plates, 8- and 16-ply-thick plates were impacted with dropped-weight impact-energy levels that correspond to the 0.05-in.-deep dent-depth barely visible impact-damage criterion that was identified previously. These specimens were then loaded to failure in compression to determine their failure loads. Many of these specimens buckled before they failed. Typical shadow moiré interferometry fringe patterns for the out-of-plane displacement contours associated with the buckling and failure modes of an undamaged 16-ply-thick flat plate are shown in Fig. 8. The contour pattern in Fig. 8(a) indicates that the plate buckled into two-half waves along its length. The plate failed at approximately

11.83 kips, and the plate failed at the plate mid-section across the plate width as shown in Fig. 8(b). These buckling and failure modes are typical for the undamaged flat plates considered in the present study. Typical out-of-plane displacement results for an impact-damaged flat plate are shown in Fig. 9. The displacement contours in Fig. 9(a) indicate that the panel buckled into three half-waves along its length, and the crest of the center buckle coincides with the impact-damage location. This buckling mode shape is different from the mode shape of the undamaged plate, and the difference is caused by the impact damage at the center of the plate. This damage causes the local stiffness of the plate to be reduced, and the damaged region acts like a hinge in the middle of the plate. The failure load for the impact-damaged plate is approximately 11.45 kips, which is approximately 3 percent lower than the failure load of the undamaged plate. The failure location for the damaged plate is at the mid-section of the plate and is through the impact-damage site as shown in Fig. 9(b).

Typical out-of-plane displacement results for an undamaged 15-in.-radius plate loaded in compression are shown in Fig. 10. The curved plate has a buckling mode with three-half waves along the length as shown in Fig. 10(a). Failure of the specimen occurred at a location that is approximately 40 percent along the length of the plate as shown in Fig. 10(b). The recorded failure load is 10.51 kips. The response of a damaged 15-in.-radius plate for an applied compression load is shown in Fig. 11. Local out-of-plane deformations in the vicinity of the impact-damage site are indicated by the moiré fringe pattern as shown in Fig. 11(a), and these deformations are representative of a locally buckled delaminated region. This plate failed at a compression load of 8.98 kips prior to buckling. The failure propagated across the plate at the mid-section as illustrated in Fig. 11(b). The failure load of the damaged 15-in.-radius curved plate is approximately 15 percent less than the failure load of the corresponding damaged flat plate. Residual-strength results for damaged and undamaged 8- and 16-ply-thick cylindrically curved plates are summarized in Fig. 12. These results indicate that the residual strength of these plates is a function of the plate radius. The 15-in.-radius plates have the most severe reduction in residual strength relative to the flat plates. The results for the 16-ply-thick curved plates indicate that the plates with radii between 30.0 and 60.0 inches have higher failure loads than the flat plates, and the plates with radii approaching 15.0 inches have lower failure loads than the flat plates.

Concluding Remarks

The results of a study of the effects of low-speed impact damage on the response of thin, cylindrically curved, graphite-epoxy plates are presented. These results include quasi-isotropic plates with different radii of curvature and different thicknesses, and the results are compared with results for the corresponding flat plates. The results of the study indicate that the contact forces for cylindrically curved plates impacted with a given impact-energy level are a function of the plate radius of curvature and thickness. Test results for an impact-energy level of 1.5 ft-lbs indicate that the magnitude of the maximum contact force developed for the curved plates decreases and then increases as the radius of the plate increases. This contact-force trend is also predicted analytically. This decreasing and then increasing trend for the contact forces associated with dropped-weight impactors is reflected in the impact-energy results for both damage initiation and for the creation of barely visible impact damage. The impact-energy levels for damage initiation in 16-ply-thick plates are different for airgun-propelled and dropped-weight impactors, but the impact-energy levels required to produce barely visible impact damage are not different. The contact forces predicted by analysis for an airgun-propelled impactor with 1.5 ft-lbs of impact energy are much greater than the corresponding forces predicted for a dropped-weight impactor, and are not influenced by the plate radius. Apparently, the response of a plate impacted by an airgun-propelled impactor is localized enough that the plate response is not affected by curvature effects.

The compression-after-impact residual-strength results for flat and curved 8- and 16-ply-thick plates suggest that these results are also a function of the plate radius. The residual strength of flat and 15-in.-radius curved plates with barely visible impact damage is approximately 3 and 15 percent less than the failure load for the corresponding undamaged plates, respectively. These results suggest that radius of curvature is an important structural parameter that must be considered when determining the damage-tolerance characteristics of thin, cylindrically curved, composite plates.

References

1. Ambur, D. R., Starnes, J. H., Jr., and Prasad, C. B., "Influence of Transverse Shear and Large Deformation Effects on the Low-Speed Impact Response of Laminated Composite Plates," NASA TM-107753, April 1993.
2. Matsuhashi, H., "Nonlinear Analysis of Composite Laminated Plates Subjected to Impact Loading," M. S.

Thesis, September 1992, Department of Aeronautics and Astronautics, Massachusetts Institute of Technology, Cambridge, MA.

3. Byun, C., and Kapania, R. K., "Nonlinear Impact Response of Thin Imperfect Laminated Plates Using a Reduction Method," *Composites Engineering*, Vol. 2, No. 5-7, 1992, pp. 391-410.

4. Palazotto, A., Perry, R., and Sandhu, R., "Impact Response of Graphite-Epoxy Cylindrical Panels," *AIAA Journal*, Vol. 30, No. 7, July 1992, pp. 1827-1832.

5. Kistler, L. S., "Experimental Investigation of the Impact Response of Cylindrically Curved Laminated Composite Plates," AIAA-94-1604-CP, April 1994.

6. Ambur, D. R., Starnes, J. H., Jr., "Influence of Large-Deflection Effects on the Impact Response of Flat and Curved Composite Plates," AIAA-95-1205-CP, April 1995.

7. Wardle, B. L., and Lagace, P. A., "Importance of Instability in the Impact Response of Composite Shells," AIAA-96-1468-CP, April 1996.

8. Ambur, D. R., and Starnes, J. H., Jr., "Nonlinear Response and Damage initiation Characteristics of Composite Curved Plates Subjected to Low-Speed Impact," AIAA-97-1058-CP, April 1997.

Table 1. Mechanical properties of AS4-3502 graphite-epoxy unidirectional tape material.

Longitudinal modulus, E_1 (Msi)	20.00
Transverse modulus, E_2 (Msi)	1.30
In-plane shear modulus, G_{12} (Msi)	0.87
Transverse shear modulus, G_{23} (Msi)	0.51
Transverse shear modulus, G_{13} (Msi)	0.87
Major Poisson's ratio, ν_{12}	0.3

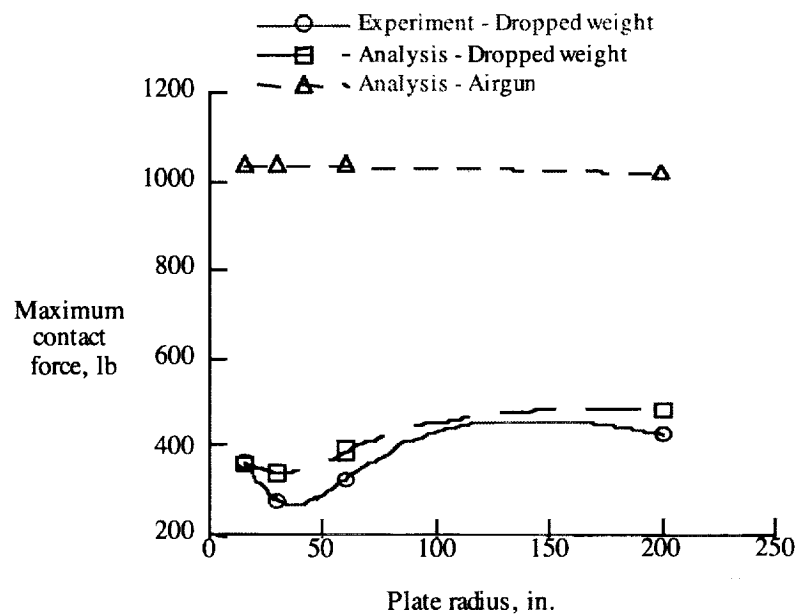


Figure 1. Contact force results for 16-ply-thick, quasi-isotropic plates impacted by dropped weights and airgun propelled impactors with 1.5 ft-lbs of impact energy.

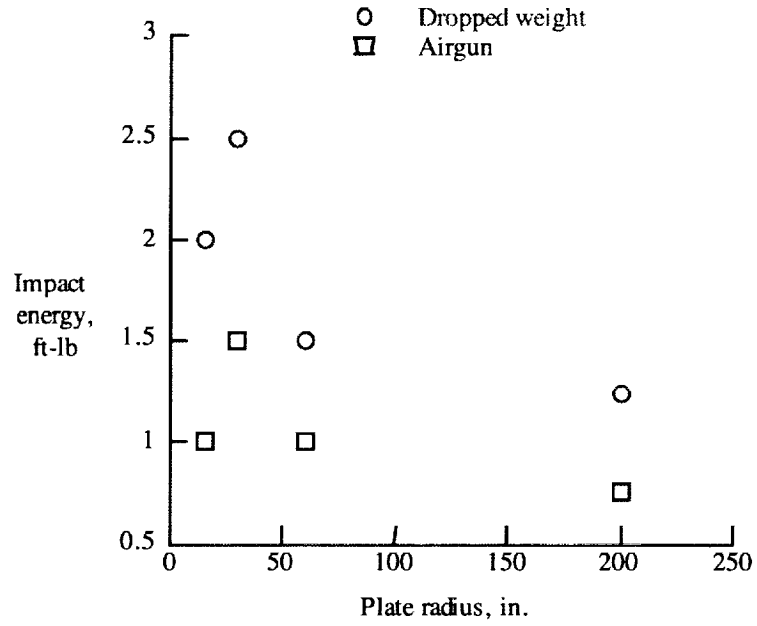


Figure 2. Damage-initiation impact energy levels for 16-ply-thick, quasi-isotropic plates impacted by dropped-weight and airgun impactors.

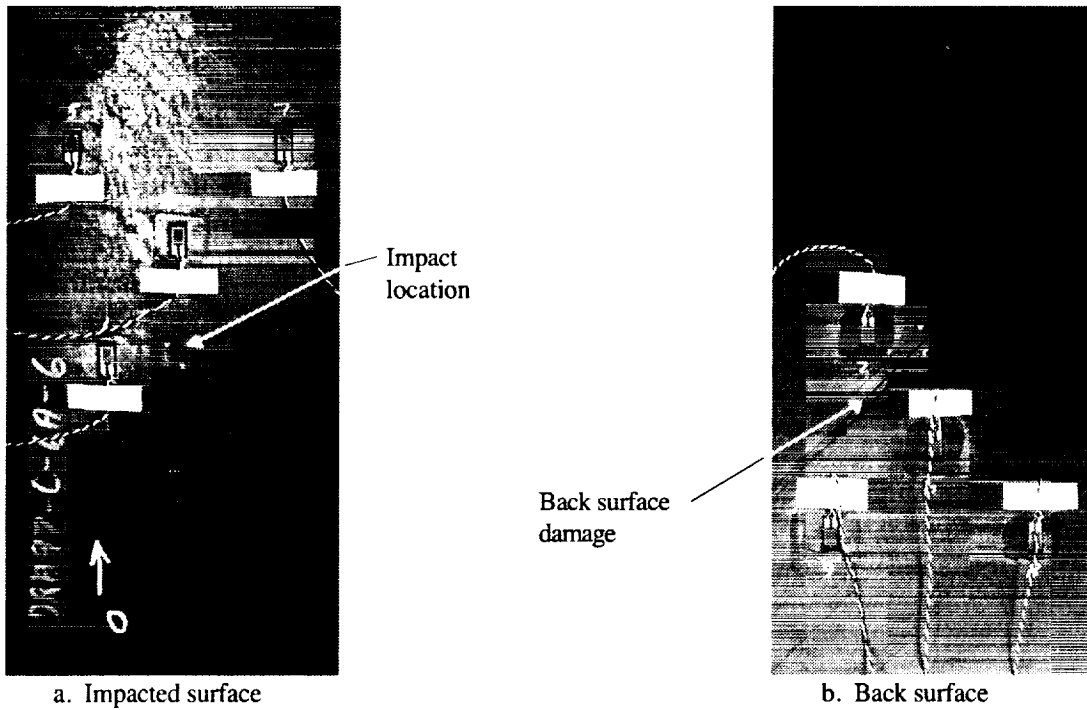


Figure 3. Photographs of a 16-ply-thick quasi-isotropic flat plates with barely visible impact damage.

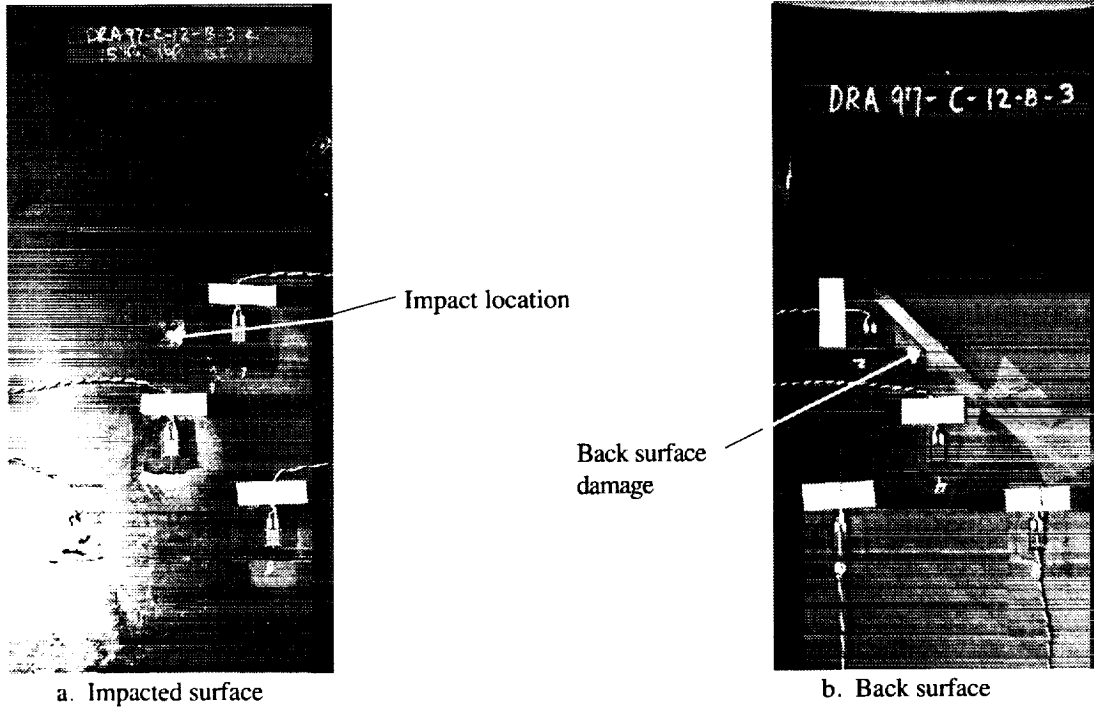


Figure 4. Photographs of a 16-ply-thick quasi-isotropic curved plate with 15-in. radius with barely visible impact damage.

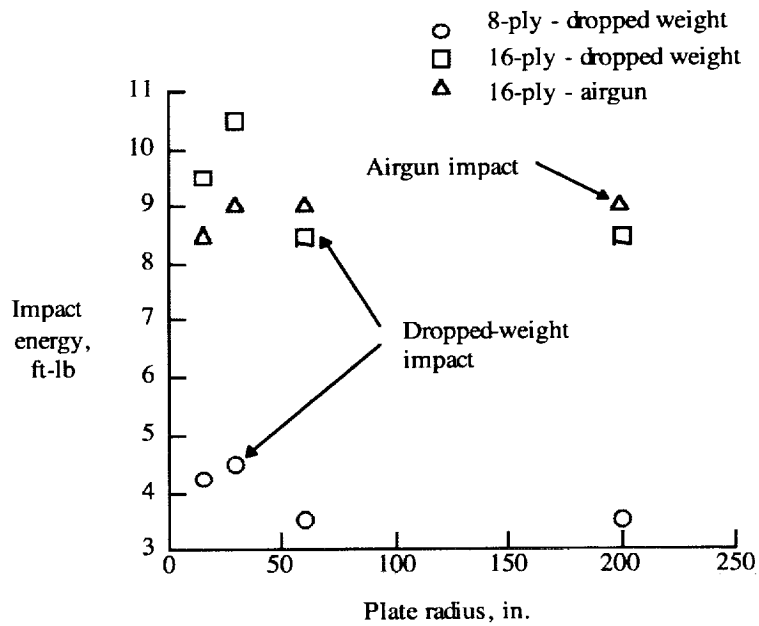


Figure 5. Dropped-weight and airgun impact-energy levels for barely visible impact damage in 8- and 16-ply-thick quasi-isotropic plates with different radii.

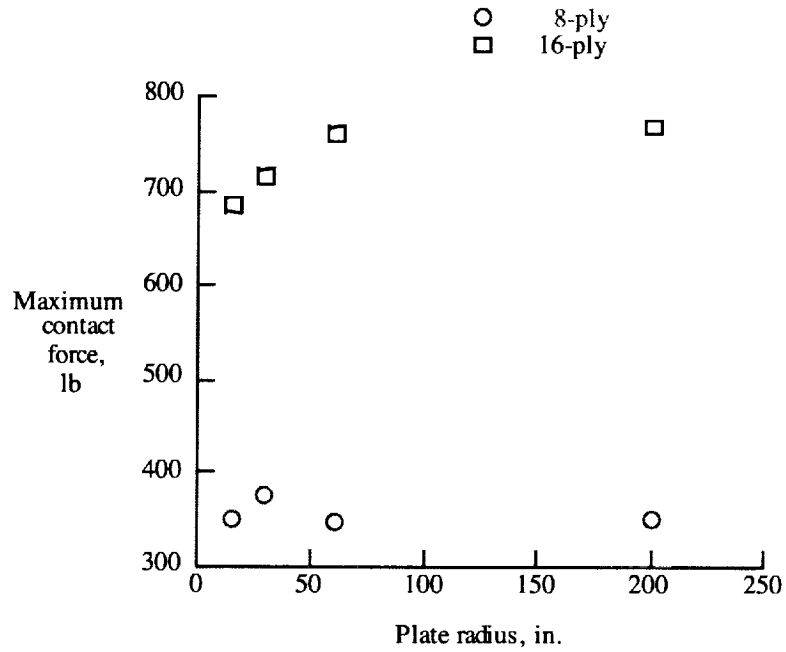


Figure 6. Maximum contact force magnitudes for dropped-weight impact-energy levels for barely visible impact damage in 8- and 16-ply-thick quasi-isotropic curved plates with different radii.

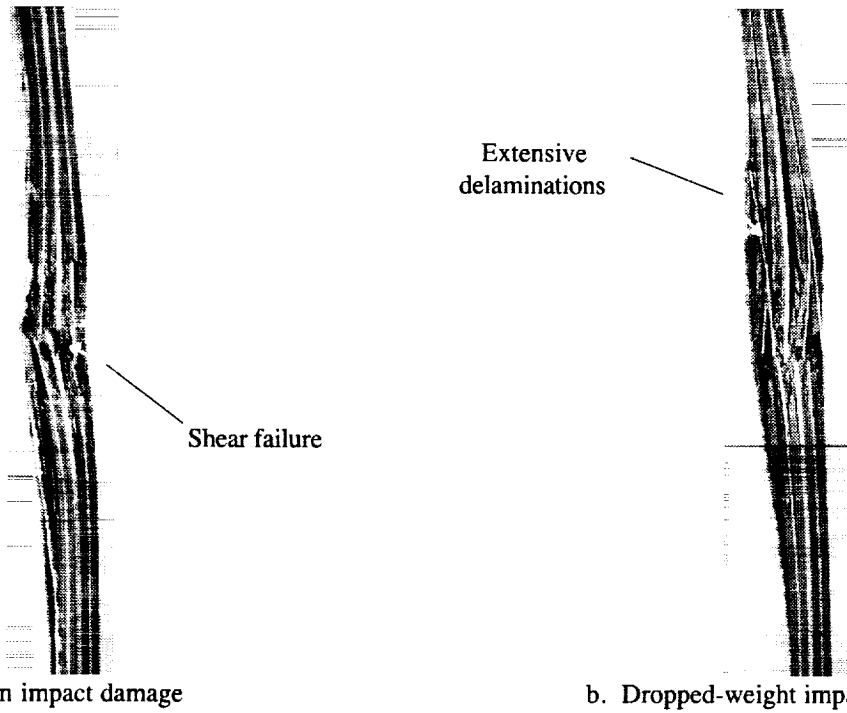
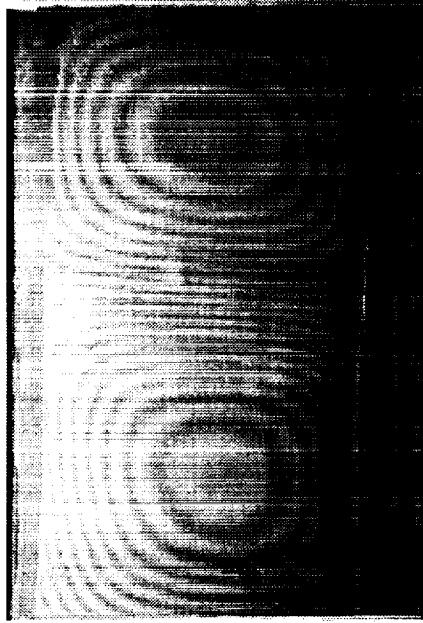
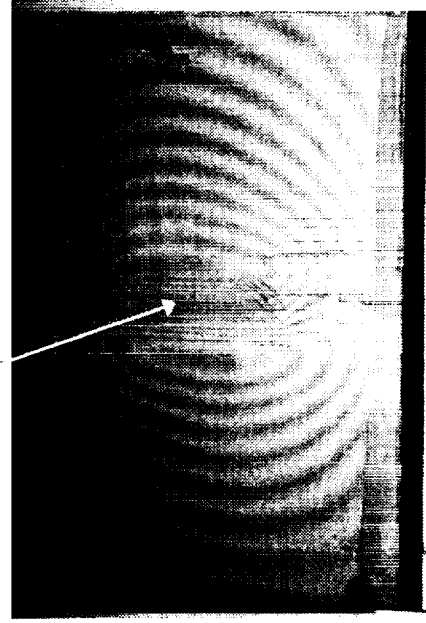


Figure 7. Photomicrographs of 16-ply-thick quasi-isotropic 15-in.-radius curved plates subjected to dropped-weight and airgun impacts with 8.5 ft-lbs of impact energy.

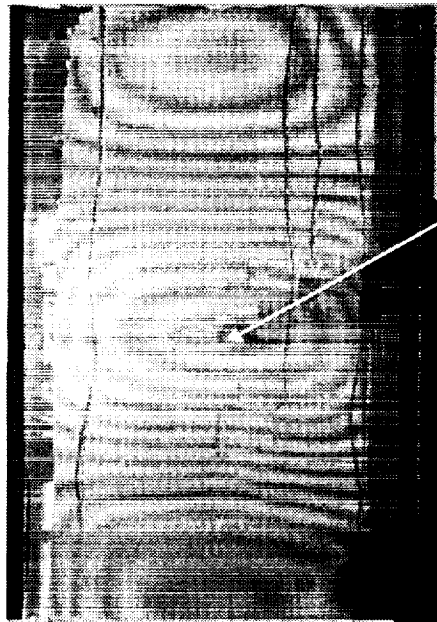


a. Buckled mode shape prior to plate failure

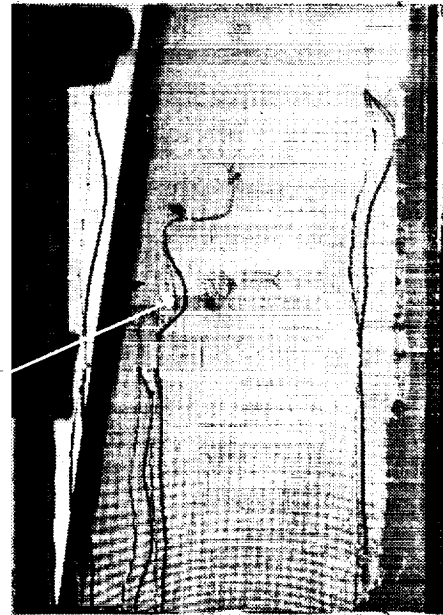


b. Plate failure through the mid-section.

Figure 8. Out-of-plane displacement contours for a compression loaded 16-ply-thick undamaged flat plate.



a. Buckling pattern with three half-waves

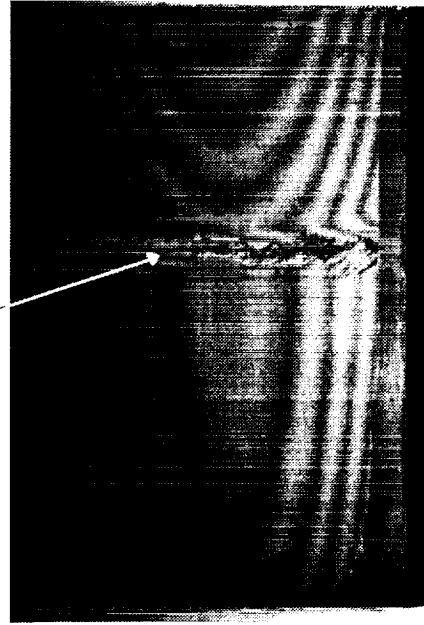


b. Failure through the damaged site

Figure 9. Out-of-plane displacement contours for a compression loaded 16-ply-thick flat plate subjected to barely visible impact damage with a dropped weight.



a. Buckling pattern with three half-waves



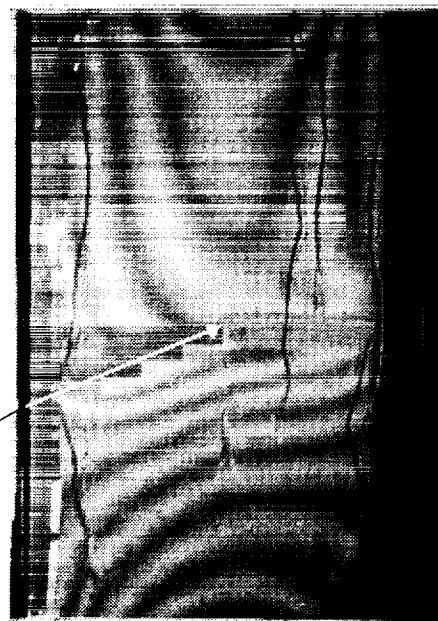
b. Off-center panel failure

Failure location

Figure 10. Out-of-plane displacement contours for a compression-loaded 16-ply-thick undamaged 15-in. radius curved plate.



a. Damage growth with no buckling

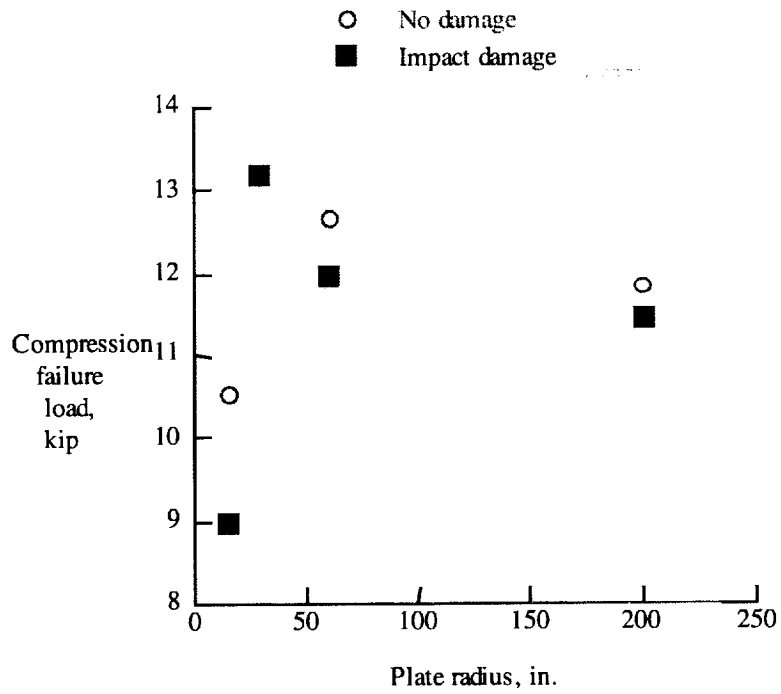


b. Failed plate

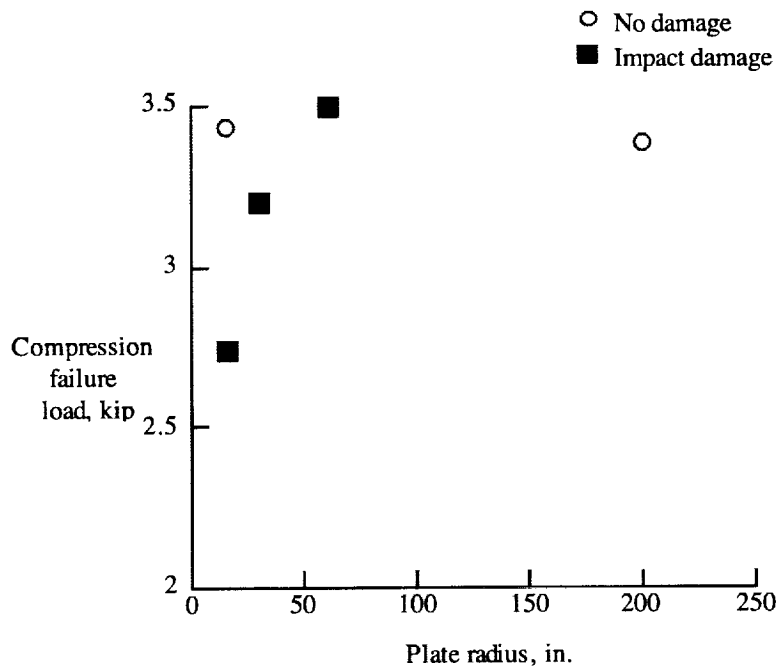
Impact damage site

Failure location

Figure 11. Out-of-plane displacement contours for a compression loaded 16-ply-thick 15-in. radius curved plate subjected to barely visible impact damage with a dropped weight.



a. 16-ply-thick curved plates



b. 8-ply-thick curved plates

Figure 12. Summary of residual strength results for curved plates with different radii.

